

FDTD SIMULATION OF COMPACT ANTENNAS FOR A GROUND-PENETRATING RADAR

Seung-Yeup Hyun, Sang-Wook Kim, and Se-Yun Kim
Imaging Media Research Center, Korea Institute of Science and Technology
P.O. Box 131, Cheongryang, Seoul, Korea
E-mail : ksy@willow.kist.re.kr

1. Introduction

GPR(ground-penetrating radar) has been used as an effective tool for detecting buried targets or geological anomalies[1]. Electromagnetic analysis of GPR is very difficult because of the close proximity of transmitting and receiving antennas, ground surface, and buried targets. These difficulties render the analysis of all elements of GPR simultaneous. Recently, electromagnetic characteristics of GPR have been analyzed by using 3-dimensional FDTD(finite-difference time-domain) method[2-5]. Those simulations include equivalent models of transmitting and receiving antennas, ground, and buried targets. In our laboratory, an improved GPR simulator was developed by adding CP(contour-path) FDTD method and extended PML condition for multi-layered media, such as air/ground. Our simulator may be applicable to the development and optimization of GPR.

The purpose of this paper is to develop a compact GPR antenna for portability using our FDTD simulator. Actual GPR measurement is also performed above PVC tank(140 cm \times 100 cm \times 20 cm) filled with dry sand in our laboratory. In FDTD simulation, the excitation of the transmitting antenna and the dielectric property of dry sand are equivalently modeled by using measured data. We compare the received voltage of GPR in FDTD simulation with measured data for the same cases.

2. FDTD simulation and results

As shown in Fig. 1, the same antennas are parallel each other above a dry sand at the height of $h_g = 2$ cm. Metallic-plate target(14.6 cm \times 14.6 cm \times 1 cm) is buried below the center of the antennas at the depth of $d_t = 5$ cm. For FDTD simulation, the excitation of the transmitting antenna is modeled by using the Gaussian pulse with a voltage peak $V_0 = 40.6262$ V and the characteristic times of rising and falling part of the pulse are given by 0.21739 ns and 0.4 ns, respectively. The electrical parameters of dry sand are modeled by approximating measured data using an open-ended coaxial probe to Debye dispersion formula ($\epsilon_{rs} = 2.72$, $\epsilon_{r\infty} = 0.846$, $\sigma_0 = 0.0029$ S/m, $\tau = 1.24$ ps). As shown in Fig. 2, the antennas in FDTD simulation are used cavity-backed and resistor-loaded planar dipoles, such as triangular-plate (so called "bow-tie") and rectangular-plate. To make small-size and light-weight antenna, the size of the metallic-cavity is restricted within 9 cm \times 14.5 cm

×3 cm. The computation region consists of cells with space step size $\Delta = I_{e,\min}/15.19 = 0.5$ cm. The simulation is performed for 3000 time steps with each size $\Delta t = \Delta/2c \approx 8.3$ ps, where c is the speed of light in free space.

VSWR characteristics of transmitting antennas are calculated over a wide range of frequencies DC–2.5 GHz, which correspond to meaningful bandwidth of the excitation. Fig. 3 shows VSWR vs. frequency. The wideband matching characteristics are improved by using rectangular-plate dipole antenna as $\text{VSWR} < 2.2$ up to 2.5 GHz. Time-domain E_y patterns at a radial distance $r = h_g + d_t = 7$ cm are also calculated at 4 angles, $\Psi = 0^\circ, 30^\circ, 60^\circ,$ and 90° . As shown in Fig. 4, the field patterns of two different dipoles resemble each other. In case of rectangular-plate dipole, however, peak-to-peak value of E_y field in the ground is about 30 V/m larger than that of triangular-plate dipole. It leads us to conclude that electromagnetic radiation into the ground is improved by employing rectangular-plate dipole instead of triangular-plate dipole.

Fig. 5 illustrates the effects of two dipole types on the received voltages in the FDTD simulation. When no target is buried, two kinds of the received voltages have the same peak-to-peak value. On the other hand, when metallic-plate target is buried, peak-to-peak value is about 0.4 V greater for rectangular-plate dipole than for triangular-plate dipole. Fig. 6 shows comparison of FDTD results and measured data for rectangular-plate dipole. The FDTD results agree well with measured data.

3. Conclusions

The transmitting and receiving characteristics of planar antennas for GPR are analyzed by using 3-dimensional FDTD method. It is found that the rectangular-plate dipole is suitable for a compact GPR antenna. In spite of no change in direct-coupling between the transmitting and receiving antennas, the rectangular-plate dipole provides lower VSWR and stronger coupling into the ground than the triangular-plate dipole. The validity of our FDTD simulation is confirmed by showing the convergence of the FDTD results to the measured data of the received voltage for GPR.

References

- [1] D. J. Daniels, *Subsurface-Penetrating Radar*. London, UK: IEE, 1996.
- [2] J. M. Bourgeois and G. S. Smith, "A fully three-dimensional simulation of a ground-penetrating radar: FDTD theory compared with experiment," *IEEE Trans. Geosci. Remote Sensing*, vol. GRS-34, no. 1, pp. 36-44, Jan. 1996.
- [3] R. L. Roberts and J. J. Daniels, "Modeling near-field GPR in three dimensions using the FDTD method," *Geophysics*, vol. 62, no. 4, July-Aug. 1997.
- [4] J. M. Bourgeois and G. S. Smith, "A complete electromagnetic simulation of the separated-aperture sensor for detecting buried land mines," *IEEE Trans. Antennas Propagat.*, vol. AP-46, no. 10, pp. 1419-1426, Oct. 1998.
- [5] Y. Nishioka, O. Maeshima, T. Uno, and S. Adachi, "FDTD analysis of resistor-loaded bow-tie antennas covered with ferrite-coated conducting cavity for subsurface radar," *IEEE Trans. Antennas Propagat.*, vol. AP-47, no. 6, pp. 970-977, June 1999.

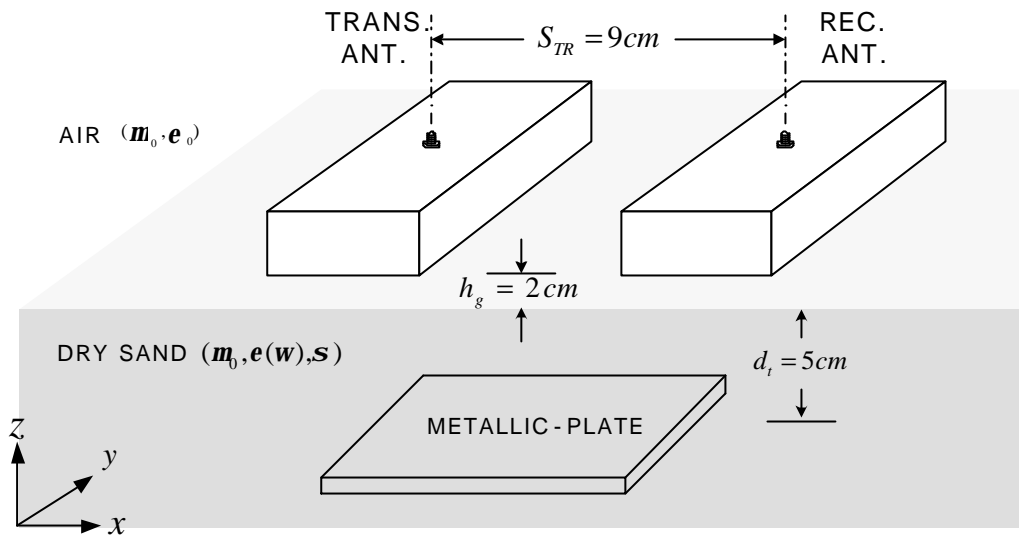
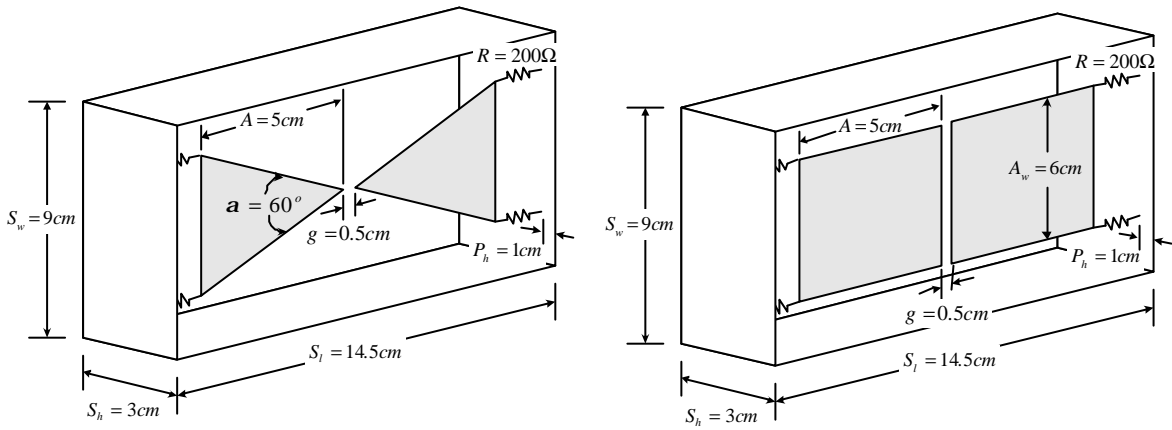


Fig. 1. Geometry of a bistatic GPR system.



(a) Triangular-plate dipole.

(b) Rectangular-plate dipole.

Fig. 2. Geometry of GPR antennas.

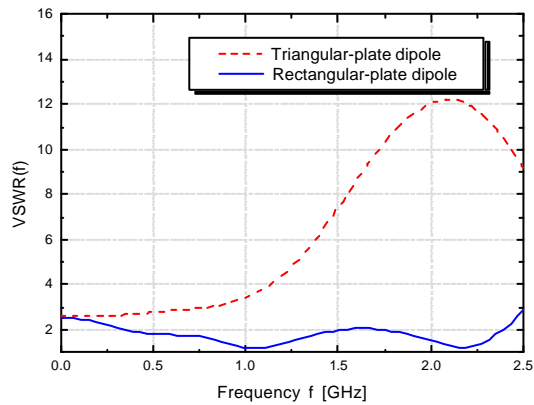


Fig. 3. Calculated VSWR as function of frequency for dipole antennas.

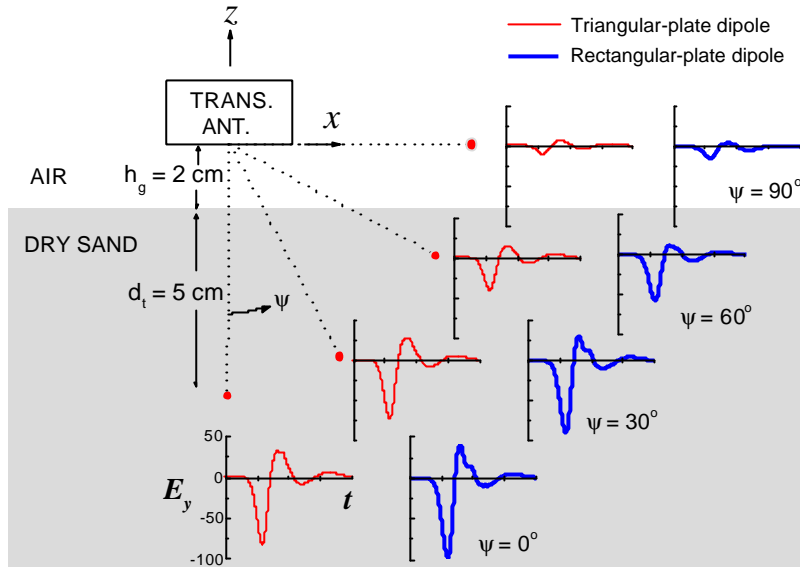
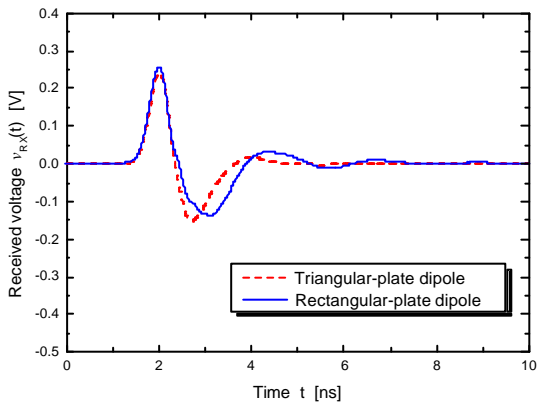
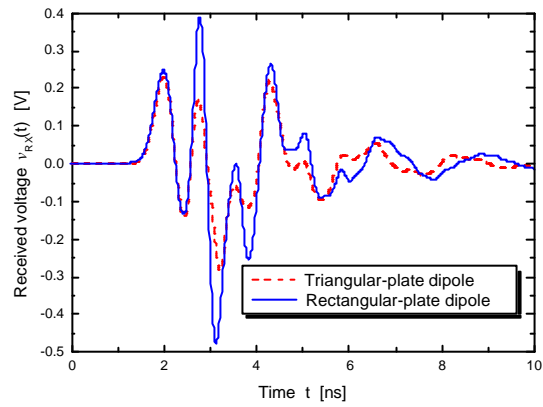


Fig. 4. Near-field E_y patterns of dipole antennas.

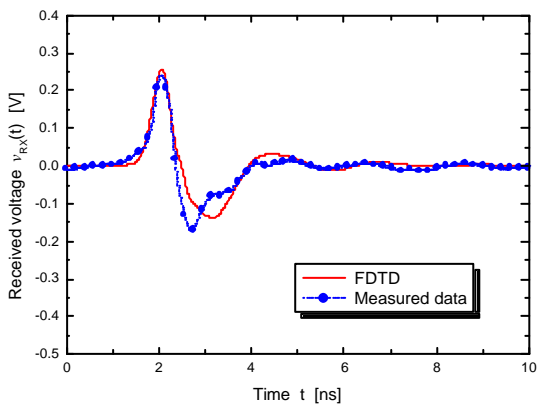


(a) No target is buried.

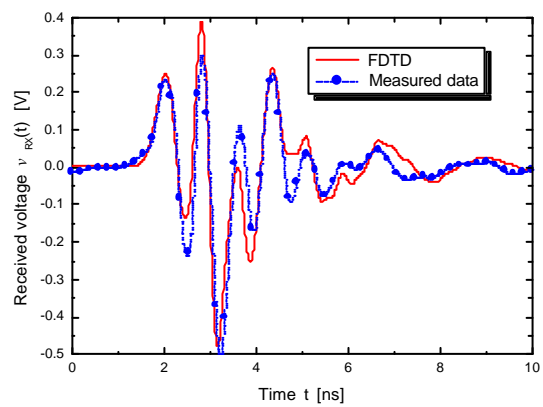


(b) Metallic-plate is buried.

Fig. 5. Received voltage of a bistatic GPR system with planar dipole antennas.



(a) No target is buried.



(b) Metallic-plate is buried.

Fig. 6. Comparison of FDTD results and measured data for rectangular-plate dipoles.